Available online at www.sciencedirect.com
ScienceDirect
Journal of Sound and Vibration 297 (2006) 842–864
JOURNAL OF SOUND AND VIBRATION
www.elsevier.com/locate/jsvi

Flow-induced oscillations of a square cylinder due to interference effects

B.H.L. Gowda[a], R. Ajith Kumar[b,*]

[a]Department of Applied Mechanics, Indian Institute of Technology Madras, Chennai – 36, India
[b]Department of Mechanical Engineering, Amrita Viswa VidyaPeetham, Ettimadai Campus, Coimbatore – 641 105, Tamil Nadu, India

Received 25 May 2005; received in revised form 29 March 2006; accepted 2 May 2006
Available online 26 July 2006

Abstract

Measurements of the flow-induced oscillations of a spring-mounted square cylinder (test cylinder, side dimension B) due to the presence of a rigid square cylinder (interfering cylinder, side dimension b) are presented. Ratios of $b/B = 0.5, 1.0, 1.5$ and 2.0 have been used. Various relative positions of the test cylinder and the interfering cylinder, in tandem, side-by-side and staggered arrangements are considered (in all of the positions considered, the interfering cylinder was never upstream of the test cylinder). The results show that under certain combinations of the b/B ratio and the relative position, the test cylinder can experience oscillatory amplitudes almost three times those observed for the no-interfering case. Under certain other conditions, the vibrations are completely suppressed. The observed features are discussed with reference to earlier related studies. Flow visualisation results are obtained by using (a) stationary test cylinder and (b) oscillated test cylinder, to provide an explanation for the observed features.

1. Introduction

Interference effects on the flow-induced vibrations of cylindrical bodies with circular cross section and prismatic bodies with square cross section are important in many practical situations such as flow around chimney stacks, tube bundles in heat exchangers, power transmission lines, off shore structures, bridge pylons, building structures etc.

There is a considerable amount of data on the flow-induced vibrations of cylinders with circular cross sections but literature shows that only limited attempts have been made on prismatic bodies with square cross section. On square cylinders, for the single cylinder case, there is enough data but comparatively less information on cases with interference. The investigations of Vickery [1], Boston and Mair [2], Otsuki et al. [3], Nakamura and Mizota [4], Parkinson [5], and Olivari [6] have dealt with single square cylinder cases wherein they have brought out various aerodynamic characteristics and forces acting on a square cylinder. Interference effects between two square cylinders in different arrangements (such as tandem, side-by-side and staggered)

*Corresponding author. Tel.: +91 422 2656422x362; fax: +91 422 2656274.
E-mail address: ajithkumar_64@yahoo.co.in (R.A. Kumar).

0022-460X/$ - see front matter © 2006 Elsevier Ltd. All rights reserved.
doi:10.1016/j.jsv.2006.05.003

Nomenclature

a	peak-to-peak amplitude
B	side dimension of the test cylinder
b	side dimension of the interfering cylinder
D	diameter of the test circular cylinder
d	diameter of the interfering circular cylinder
f	fundamental natural frequency of the spring-cylinder system
k_s	scruton number: mass damping parameter ($2m\delta/\rho B^2$)
L	longitudinal spacing between axes of cylinders
M	magnification factor
m	mass per unit length of the test cylinder
T	transverse spacing between axes of cylinders
U	free stream velocity
ρ	density of air
δ	logarithmic decrement

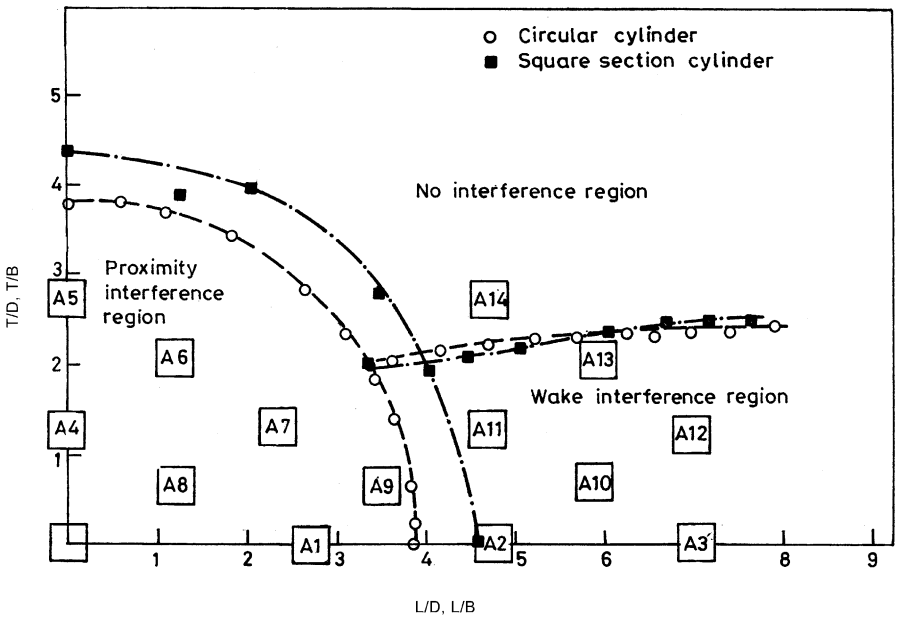

Fig. 1. The various flow regions and arrangements tested (for circular cylinder, results are adopted from Zdravkovich [11]).

were investigated by Blessmann and Riera [7], Sakamoto et al. [8], Takeuchi and Matsumoto [9] and Bailey and Kwok [10].

The studies of Zdravkovich [11] deal with the flow-induced oscillations of two interfering circular cylinders when both are elastically mounted and placed at various relative positions. These relative positions have been identified based on the flow field around two rigid cylinders in various arrangements and are shown in Fig. 1. Gowda et al. [12–14] have studied the interference effects when one of the circular cylinders is spring-mounted and the other is rigid. In the present investigation, detailed flow visualisation studies were conducted using two rigid square cylinders to identify the interference regions for the square cylinder and it was found that these regions are almost the same as those for circular cylinder except that the proximity interference region for the square cylinder is slightly larger compared to the circular cylinder (Fig. 1). Hence, for the square cylinder also, the same relative positions as those with circular cylinder were considered for investigation. In the studies reported in what follows, the vibratory response of an elastically mounted square cylinder (test cylinder) over the entire resonance range was investigated, as caused by the interference effects of a rigid square cylinder placed at various positions in the interference regions as shown in Fig. 1. The response of the test cylinder was obtained for different ratios of interfering cylinder side dimension b to the test cylinder side dimension B: i.e.,

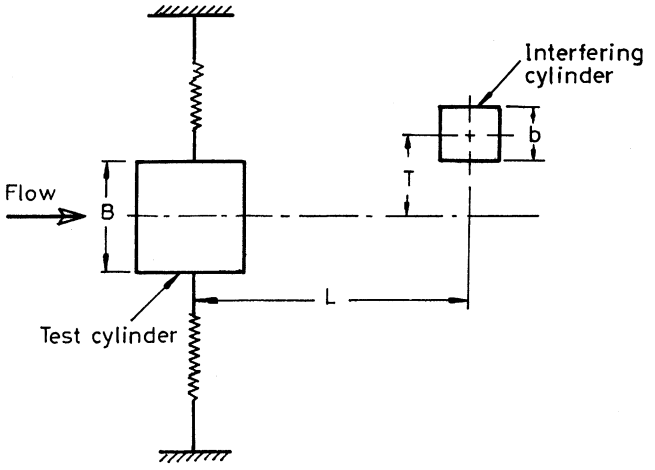

Fig. 2. The configuration tested. Cases studied: $b/B = 0.5, 1.0, 1.5, 2.0$.

$b/B = 0.5, 1.0, 1.5, 2.0$ (see Fig. 2). The reduced velocities considered are in the vortex excitation range and slightly beyond it. The mechanisms of excitation and the corresponding flow fields in the various regions are also described.

2. Experimental set-up

The arrangement is essentially the same as that used by Gowda et al. [12–14]. The experiments were conducted on an aluminium tube with a square cross section of side 12 mm, wall thickness 1 mm, length 140 mm. The cylinder was positioned vertically at the centre of a rectangular frame supported by four springs. The frame was positioned in front of an open circuit wind tunnel with a square exit duct measuring 120 mm × 120 mm such that the cylinder was at a distance of 44 mm from the exit of the tunnel. The velocity is uniform over the 70% of the exit cross section (variation is less than 1%) and reduces gradually towards the edges.

One of the springs supporting the cylinder was connected to a dynamic pick up (Type 8001, Bruel and Kjaer). The pick up was in turn connected to a storage oscilloscope (Type 1744A, Hewlette Packard) through a charge amplifier (Type 2626, Bruel and Kjaer). The cylinder was capable of vibrating in a direction transverse to the oncoming flow. The natural frequency and the logarithmic decrement of the spring-mounted cylinder were determined to be 54 Hz and 0.00368, respectively. The mass damping parameter k_s (Scruton number) was equal to 3.2 (a list of nomenclature is given). The natural frequency (f) and logarthmic decrement of the system are found by the free vibration method. The test cylinder along with the frame is mounted horizontally in a rigid stand and weight is attached to it through a thin thread. The thread is snapped and the ensuing oscillations are stored in an oscilloscope from which the natural frequency is determined. The trace of the exponentially decreasing amplitude against time under free vibration of the test cylinder is used in finding the logarithmic decrement (δ). Stiffness (k) of the system is found out by noting down the deflection of the cylinder in this horizontal position, when known weights are added in a pan which is tied to the centre of the cylinder. The deflection of the cylinder is measured by using a needle which is stuck horizontally over the centre of the cylinder and moves against the surface of a graduated scale placed behind the cylinder. Natural frequency of the system obtained as mentioned earlier is checked by using the formula, $\omega n = \sqrt{(k/\mathrm{Mc})}$ where 'Mc' is the total mass of the test cylinder. The natural frequency of the system is rechecked by subjecting the test cylinder to vortex induced oscillations and recording these oscillations in the storage oscilloscope.

The interfering cylinders used for tandem and staggered arrangement were made out of solid aluminium rods with a smooth finish and square cross section. They were each of length 140 mm and side dimension ratios (b/B) of 0.5, 1.0, 1.5 and 2.0 were used. For side-by-side arrangement, a different set of cylinders of the same relative dimensions as for tandem and staggered arrangements were used. These cylinders were 120 mm

long and could be conveniently placed besides the test cylinder. Further details of the test set-up have been given by Gowda and Prabhu [12]. The response of the test cylinder without any interference was first determined. Then the interference studies were carried out by varying the flow velocity covering the entire resonance range. The range of Reynolds number referred to the test cylinder side dimension is between 3000 and 11000.

3. Results

3.1. Single cylinder

Before carrying out the interference studies, the response of the test cylinder without any interfering body was obtained and is shown in Fig. 3. In this figure (as also in other figures), the variation of non-dimensional amplitude (a/B) with reduced velocity (U/fB) is plotted. The lock-in region observed is $7.3 \leqslant U/fB \leqslant 14.0$. Vortex lock-in is observed to start at a reduced velocity of 7.30. This corresponds to a Strouhal number of 0.137 which is in good agreement with earlier investigators (e.g., [15,17]). The peak amplitude of vibration observed $[(a/B)_{\max}]$ is 0.32. The maximum amplitude remains nearly the same over a small range of reduced velocities between 9.6 and 11.0. The lock-in ceases at a reduced velocity of 14.0. The amplitude of vibration is negligibly small to the left of the 'resonance hill' and relatively small to the right of it. Hysterisis is found to be negligible as shown in Fig. 3.

A very interesting feature noticed in the vibratory response of the test cylinder is its multiple amplitudes within a low and a high peak as depicted in Fig. 3. The test cylinder (square) amplitude was observed to vary from a minimum to a maximum value, sometimes having a halt at an intermediate amplitude position from where it goes to the maximum amplitude position and vice versa. Some other times, it varies from the minimum amplitude position to the maximum without any intermediate halt. There was no regular frequency noticed in the above-mentioned switch from one amplitude level to the other. What is shown in Fig. 3 is the minimum and the maximum values of vibration amplitudes reached.

The resonance range obtained is comparable to that observed by Bearman and Obasaju [18]. They have observed that the reduced velocity range corresponding to vortex resonance is $7.0 \leqslant U/fB \leqslant 12.0$, with the maximum non-dimensional amplitude of vibration value of 0.25 for a square section cylinder. However, they have not reported the multiple amplitudes as observed in the present study. This might be due to the difference in the value of Scruton number and the other experimental conditions between the investigations.

The response curve for an isolated circular cylinder obtained by Gowda and Sreedharan [14] is also included in Fig. 3 for comparison. It is very interesting to observe the differences in the nature of the response between the two. The resonance for the circular cylinder starts at around a reduced velocity of 5 (as Strouhal number is around 0.2), whereas it begins at a value of $U/fB = 7.3$ for the square cylinder (Strouhal number = 0.137). The lock-in region for the square section is wider with higher peak amplitude of oscillation; also there is a flatter peak. The other major difference is the multiple amplitudes observed for a square cylinder, unlike the circular one. The reason for such a vibratory response (i.e., the multiple amplitudes of vibration) of the square cylinder can be explained as follows.

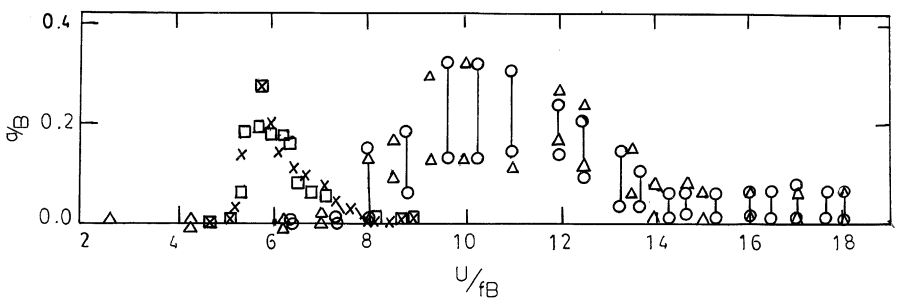

Fig. 3. The response of the test cylinder without interference. ○, velocity increasing: △, velocity decreasing (square cylinder); □, velocity increasing: ×, velocity decreasing (circular cylinder [14]).

For the square cross section, unlike for the circular geometry, while in vibration, the influence of change in the effective angle of flow incidence on the flow field around the cylinder can be expected to be considerable. The configuration of the shear layers separating from the sharp corners of the square section continuously change as observed by Obasaju [19]. This brings about changes in the characteristics of flow separation bubble and its interaction with the vortex formation as revealed by Laneville and Lu Zhiyong [20] leading to bi-stable flow conditions and consequent multiple amplitudes of vibration.

Further supportive argument to this phenomenon is provided by Luo et al. [21] in which they dealt with the change in the configuration of shear layers (with respect to the corresponding sides) as the square section cylinder vibrates. This leads to variations in the suction forces generated on the side surfaces and hence, in the vibrations. Fig. 7 of the paper by Parkinson [22] typically shows the pressure variation brought about by the change in the position of the shear layers (top and bottom) with respect to the corresponding sides due to the change in the flow angle of incidence. However, the explanations given for the occurrence of multiple amplitudes are of tentative nature and the exact reasons for the observed behaviour is yet to be understood.

3.2. Interference effects

The interference studies were carried out by placing the interfering cylinder at various positions in the different regions identified as in Fig. 1: i.e., in the proximity region, wake interference region and the region of no-interference. The locations of these positions were identified, as described earlier. The results for square cylinder (a/B versus U/fB) are presented in Figs. 4–7. In an attempt to bring out the influence of geometry, the results for circular cylinder given by Gowda and Sreedharan [14] and Sreedharan [23] are also incorporated in these figures, for comparison. The Scruton number is nearly the same for both i.e., k_s (square) = 3.2 and k_s (circular) = 3.25. The results have been obtained for $b/B = 0.5$, 1.0, 1.5 and 2.0. As in the single cylinder case, multiple amplitudes were observed for the cases with interference also.

3.2.1. Results for $b/B = 1.0$

The results for $b/B = 1.0$ are shown in the set of Figs. 4(a)–(n). In these figures (and also in others), the multiple amplitude points have been joined by vertical lines and also, the maximum amplitude points for single cylinder case have been introduced in order to bring out the interference effects more clearly. The response of the test cylinder is much different under interference conditions from that without interference (Fig. 3). The peak amplitudes, the resonance range, the mode of variation of amplitudes within the resonance range were all affected by the interference effects. Some of the features are highlighted in what follows.

Positions A1–A3 (Figs. 4(a)–(c)) refer to the tandem arrangement. At A1 and A2, the maximum amplitudes are nearly one and a half times that for the no-interference case (Fig. 4(a)). For the position A3 also, the maximum amplitude is higher than that of the no-interference case. For all the above cases, the amplitudes beyond the peak are in general, larger than those for the no-interference case along with a shift of the peak amplitude towards higher reduced velocity value. In the arrangements A1 and A3, resonance starts approximately at the reduced velocity of 8.0, whereas for position A2, it starts at $U/fB = 7.3$ (same as that of the single cylinder case). As the tandem distance increases (from A1 to A3), it can be seen that the trend in amplitude variation becomes more and more sharper (less flatter). Circular cylinder (with interference) also exhibits considerably higher amplitudes, with the resonance onset occurring at a higher value of reduced velocity compared to the single circular cylinder case (Fig. 4(a)). There is also a corresponding shift in the peak amplitudes towards higher values of U/fB similar to the square cylinder. At position A1, circular cylinder exhibits considerably higher amplitude value than the square cylinder and for the other tandem positions A2 and A3, the peak amplitude values with interference are almost the same for both of them.

In the side-by-side arrangements A4 and A5 (Figs. 4(d) and (e)), the responses are different. For square cylinder, at position A4, the vibrations are completely suppressed whereas, circular cylinder exhibits notable amplitudes but reduced when compared to its no-interference case (Fig. 4(a)). At position A5, the square cylinder exhibits considerable amplitude values with maximum amplitude (occurring at $U/fB = 10.0$) slightly higher than that of no-interference case (Fig. 4(a)). The resonance range is shifted towards lower reduced velocity range; circular cylinder exhibits reduced amplitude values at this position, lower than that of square cylinder. In this case, beyond $U/fB = 10.0$, the amplitude value steeply reduce when compared to

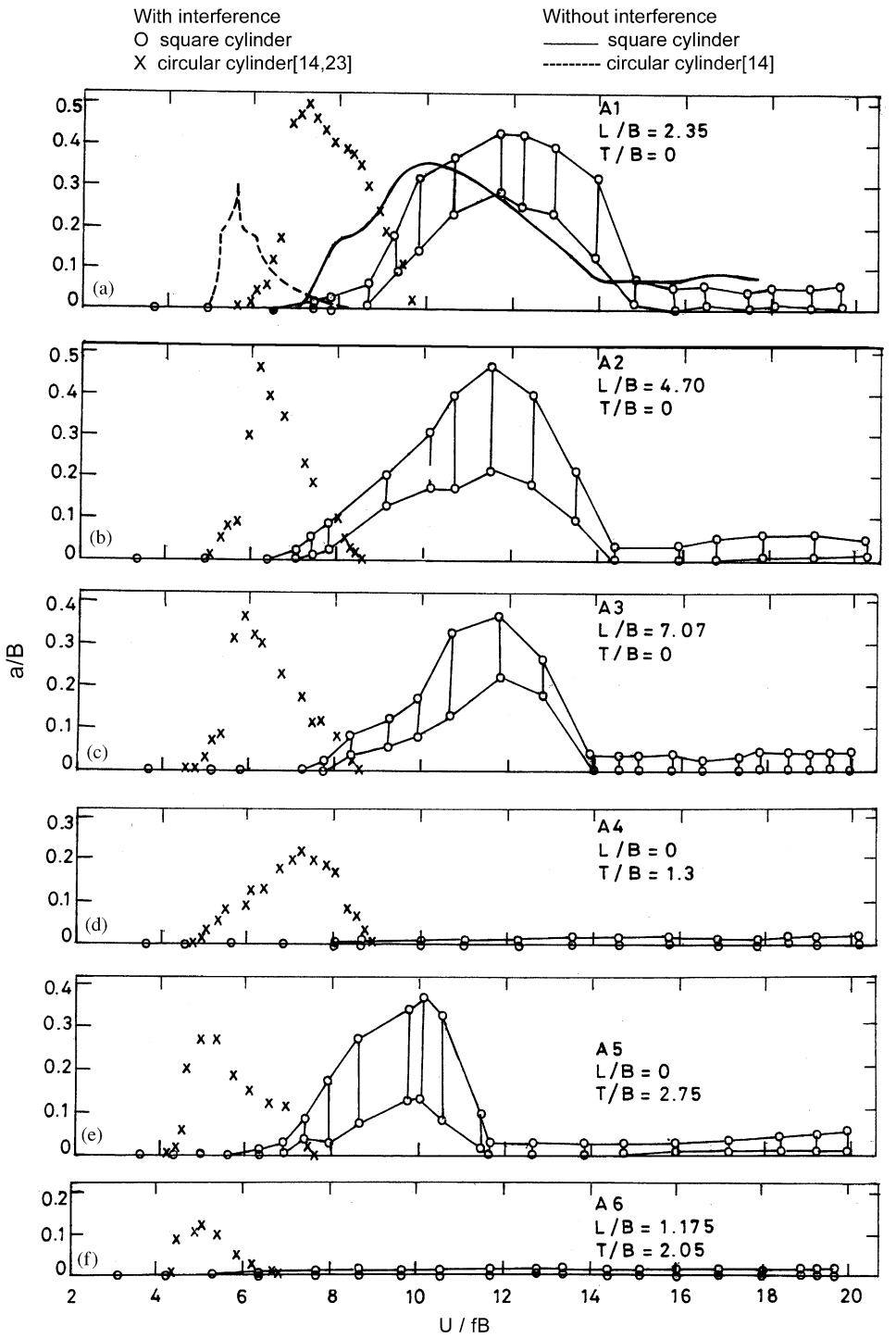

Fig. 4. Interference effects: $b/B = 1.0$. Reference position (see Fig. 1). L/B, T/B: (a) A1, 2.35, 0; (b) A2, 4.7, 0; (c) A3, 7.07, 0; (d) A4, 0, 1.30; (e) A5, 0, 2.75; (f) A6, 1.175, 2.05; (g) A7, 2.35, 1.30; (h) A8, 1.175, 0.65; (i) A9, 3.53, 0.65; (j) A10, 5.90, 0.65; (k) A11, 4.70, 1.30; (l) A12, 7.07, 1.30; (m) A13, 5.90, 2.05; (n) A14, 4.70, 2.75.

no-interference case, for square cylinder. Also, the lock-in starts early when compared to the single cylinder case at this position (A5).

Arrangements A6, A7, A8 and A9 (Figs. 4(f)–(i)) are in the 'proximity region' with the interfering cylinder located in staggered position with respect to the test cylinder. The vibrations of the test cylinder at position A6

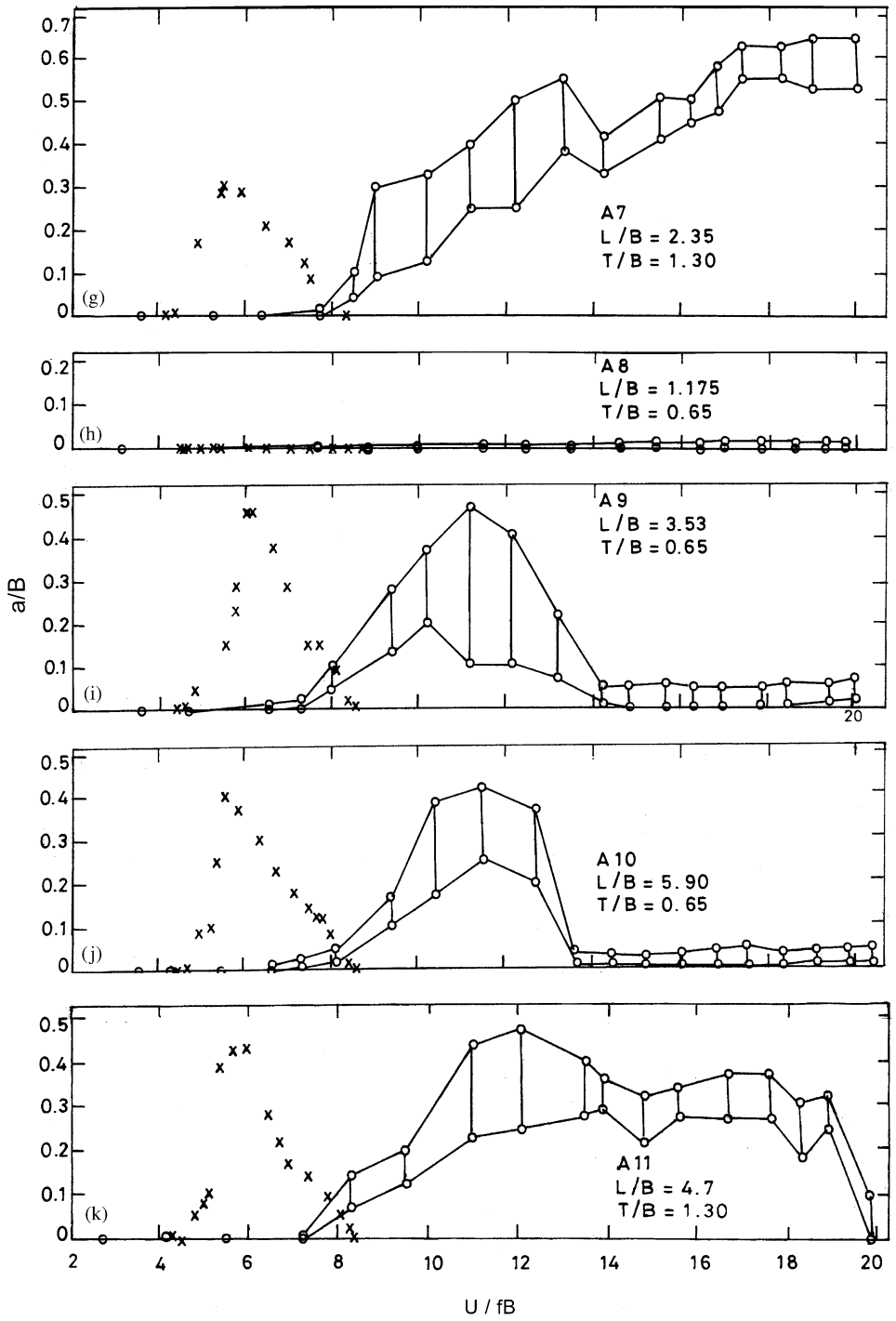

Fig. 4. (*Continued*)

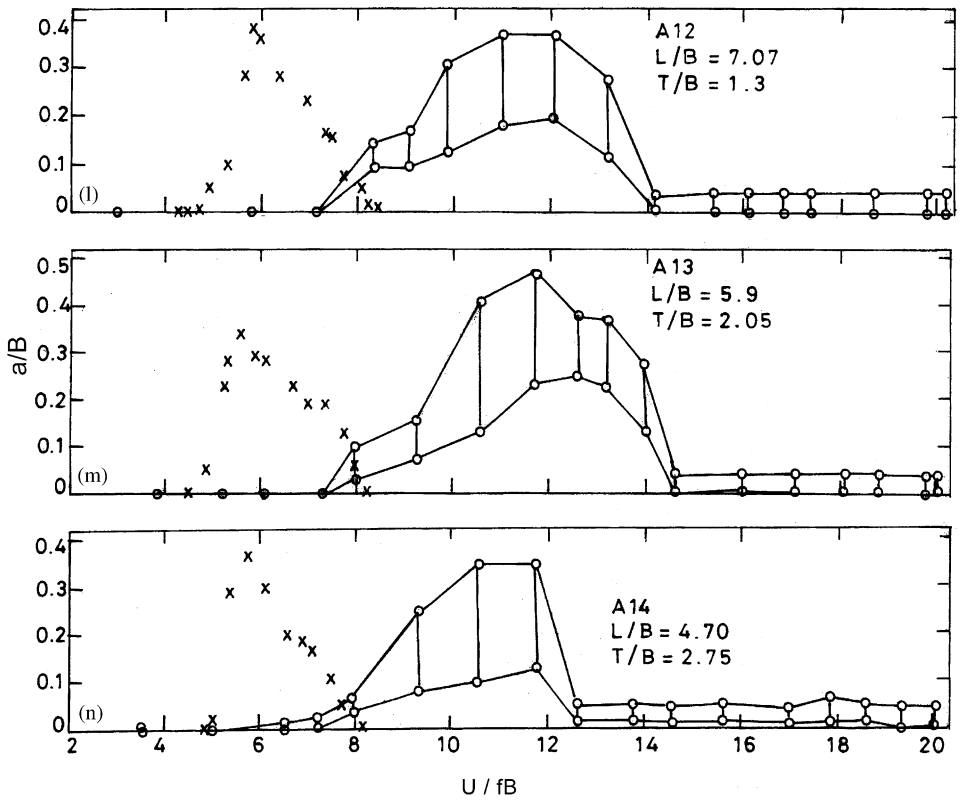

Fig. 4. (*Continued*)

(Fig. 4(f)) are completely suppressed; whereas, circular cylinder exhibits considerably reduced amplitudes. But at position A7 (Fig. 4(g)), the test cylinder shows a different type of response with amplitude reaching considerably larger values compared to the single cylinder case, particularly for $U/fB > 13.0$. Once initiated, the amplitude shows a continuously increasing trend as shown in Fig. 4(g). For circular cylinder, the amplitude is slightly higher and resonance range broader than its no-interference case (Fig. 4(a)). The maximum amplitude and the mode of variation observed is much different from that of the square cylinder. At A8 (Fig. 4(h)), the test cylinder vibrations are completely suppressed for square cylinder (same occurs for circular cylinder also). At A9 (Fig. 4(i)), both the square and circular cylinders exhibit considerable amplitudes (maximum amplitudes are almost the same for both) with the positions corresponding to their peak amplitude shifted towards higher U/fB value when compared to the respective no-interference cases.

The positions A10–A13 are located in the wake-interference region (Fig. 1) and the response characteristics of the test cylinder at these locations are shown in Figs. 4(j)–(m). At position A10 (Fig. 4(j)), the test cylinder with interference exhibits characteristics very similar to the single cylinder case but with somewhat increased magnitudes in the resonance range ($8.0 \leqslant U/fB \leqslant 13.0$). The response of test cylinder at position A11 (Fig. 4(k)) is quite different from the response at other positions. The amplitude variation follows an increasing-decreasing trend in the reduced velocity range $7.2 \leqslant U/fB \leqslant 20.0$, with a dip at $U/fB = 15.0$. Even at $U/fB = 20.0$, small but notable amplitude persists. At A12 and A13 (Figs. 4(l) and (m)), amplitude variation in general follows an increasing-decreasing trend with higher maximum amplitudes than that of the no-interference case.

In the positions aforementioned (A10–A13), in general, circular cylinder oscillates at considerably higher amplitudes (than its no-interference case), with maximum amplitudes nearly equal to that of square cylinder except for position A13 (where the maximum amplitude is lesser than that of the square cylinder). The results presented in Figs. 4(j)–(m) show that the interfering cylinder considerably influences the oscillatory response of the test cylinder even for sufficiently large distances. The maximum amplitude value and the resonance

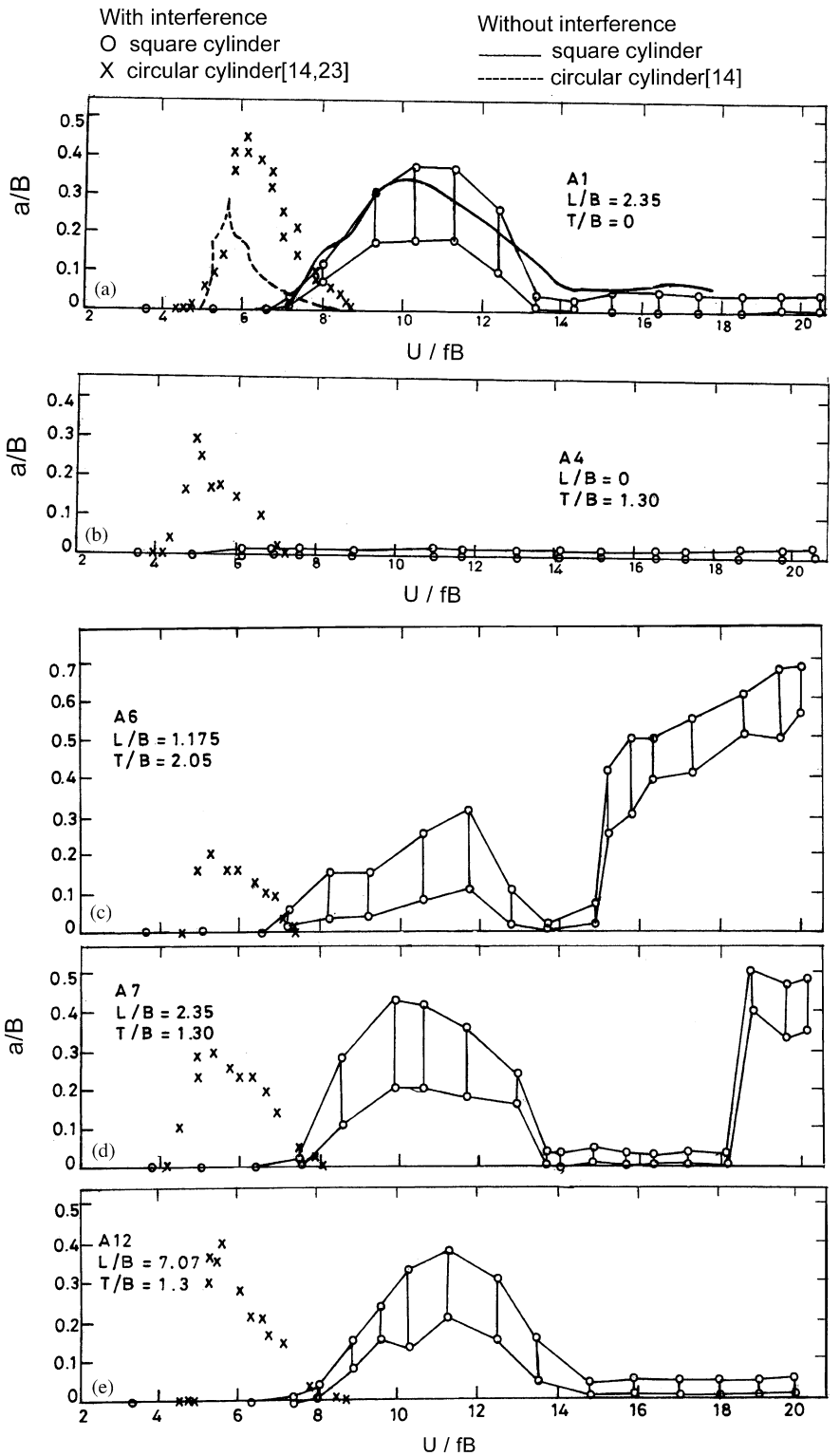

Fig. 5. Interference effects: $b/B = 0.5$. Reference position (see Fig. 1), L/B, T/B: (a) A1, 2.35, 0; (b) A4, 0, 1.30; (c) A6, 1.175, 2.05; (d) A7, 2.35, 1.30; (e) A12, 7.07, 1.30.

range are all affected due to the interference effects. Even at A14 (located in the no-interference region), it can be seen that the interference effects are not negligible (Fig. 4(n)). Here (i.e., at A14), the lock-in ceases early when compared to single cylinder case (Fig. 4(a)).

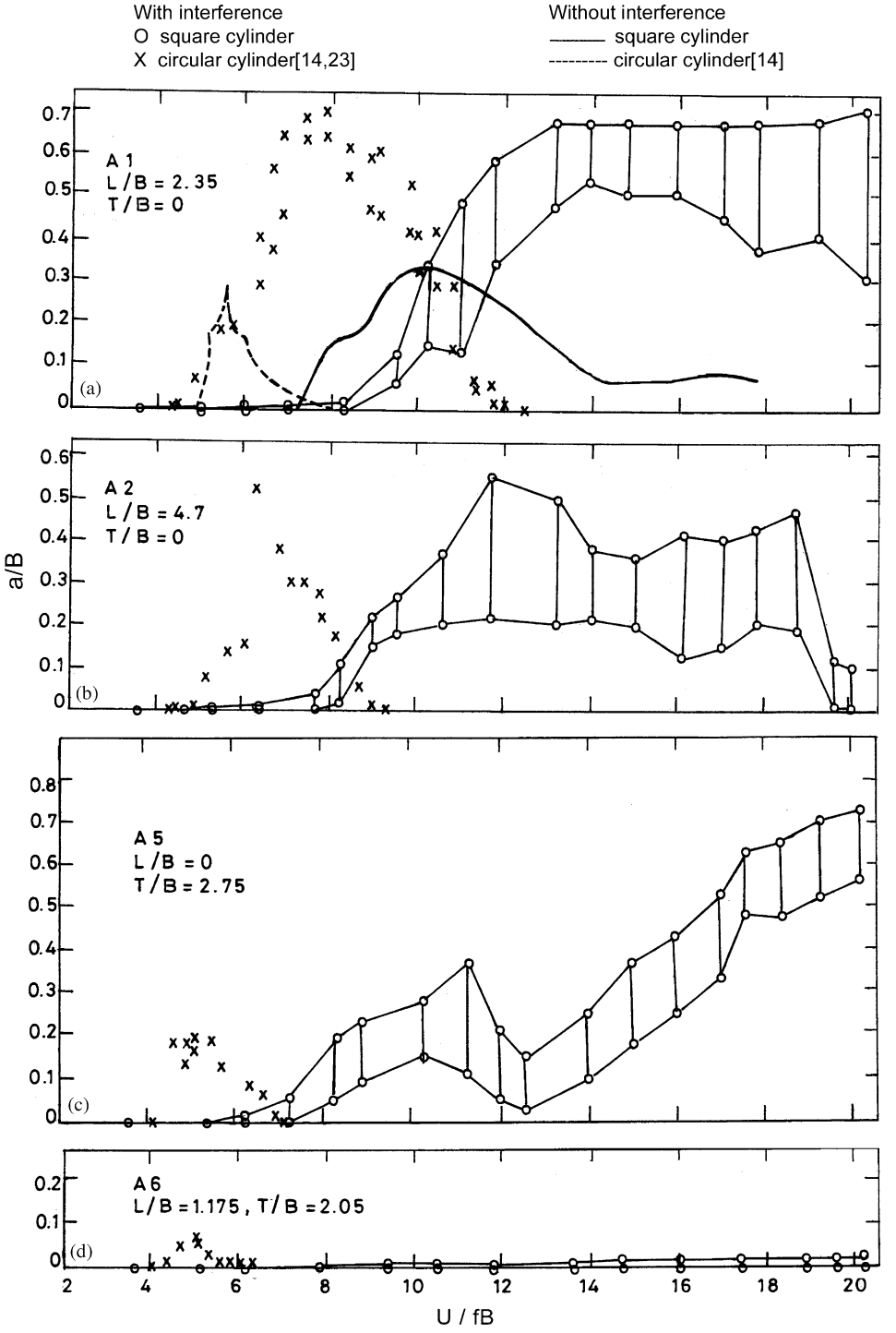

Fig. 6. Interference effects: $b/B = 1.5$. Reference position (see Fig. 1), L/B, T/B: A1, 2.35, 0; (b) A2, 4.7, 0; (c) A5, 0, 2.75; (d) A6, 1.175, 2.05; (e) A7, 2.35, 1.30; (f) A11, 4.70, 1.30; (g) A14, 4.70, 2.75.

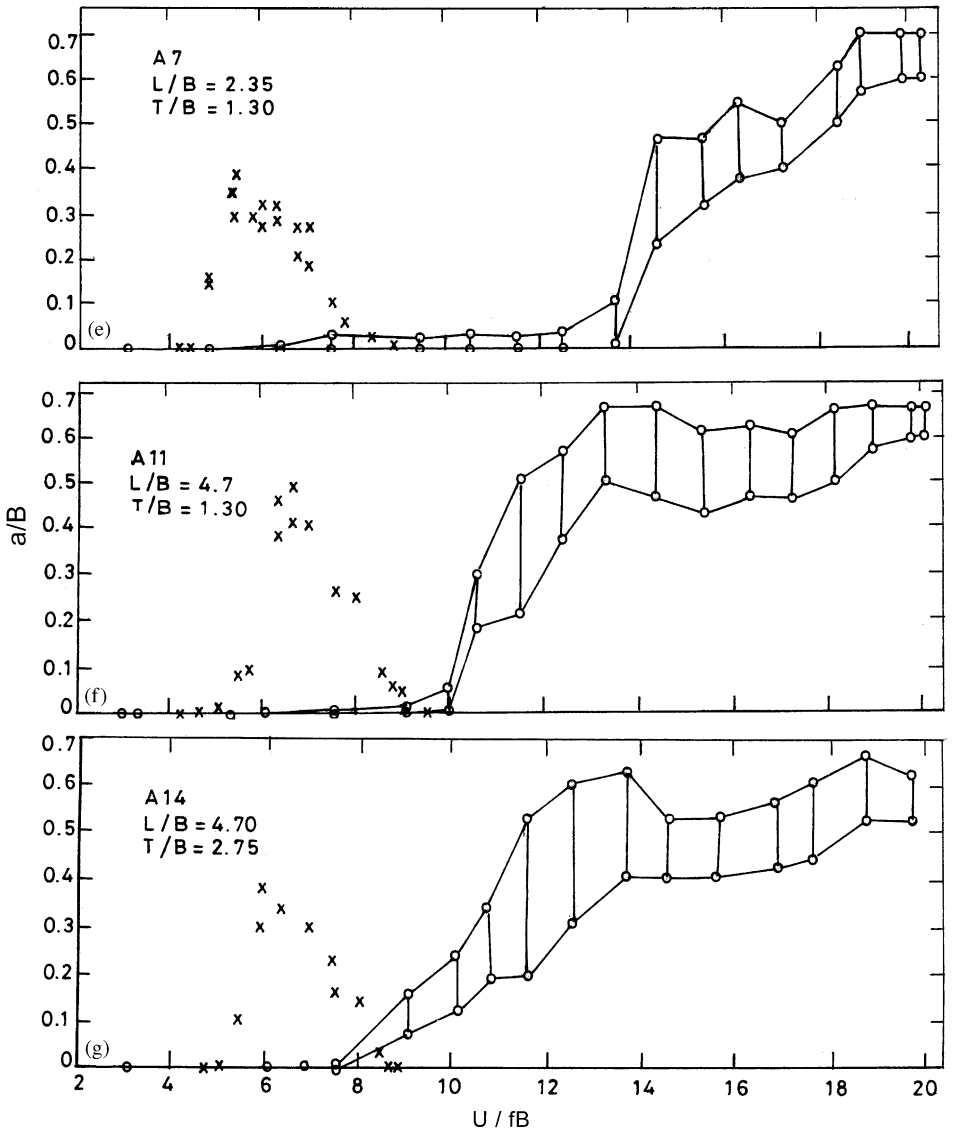

Fig. 6. (*Continued*)

The results for $b/B = 0.5$, 1.5 and 2.0 are shown in Figs. 5–7 respectively. For these cases, the results are not shown for all the arrangements, but only at some typical positions in the various regions indicated in Fig. 1.

3.2.2. Results for $b/B = 0.5$

For $b/B = 0.5$, for the tandem position A1 (Fig. 5(a)), presence of interfering cylinder has caused the test cylinder to exhibit higher amplitudes (compared to the no-interference case). Moreover, the maximum amplitude is observed to have undergone a slight shift towards higher U/fB value (when compared to its no-interference case). At this tandem location, due to interference, circular cylinder also exhibits considerable amplitudes comparable to those of square cylinder. At the side-by-side arrangement A4 (Fig. 5(b)), the test cylinder vibrations are completely suppressed due to the presence of the interfering cylinder; whereas, circular cylinder exhibits oscillations with maximum amplitude value quite comparable to that of it's no-interference case (Fig. 5(a)). In the staggered arrangement, at position A6, the amplitude exhibits a continuously increasing trend after an increasing-decreasing profile as shown in Fig. 5(c). Even at $U/fB = 20$, very high amplitude

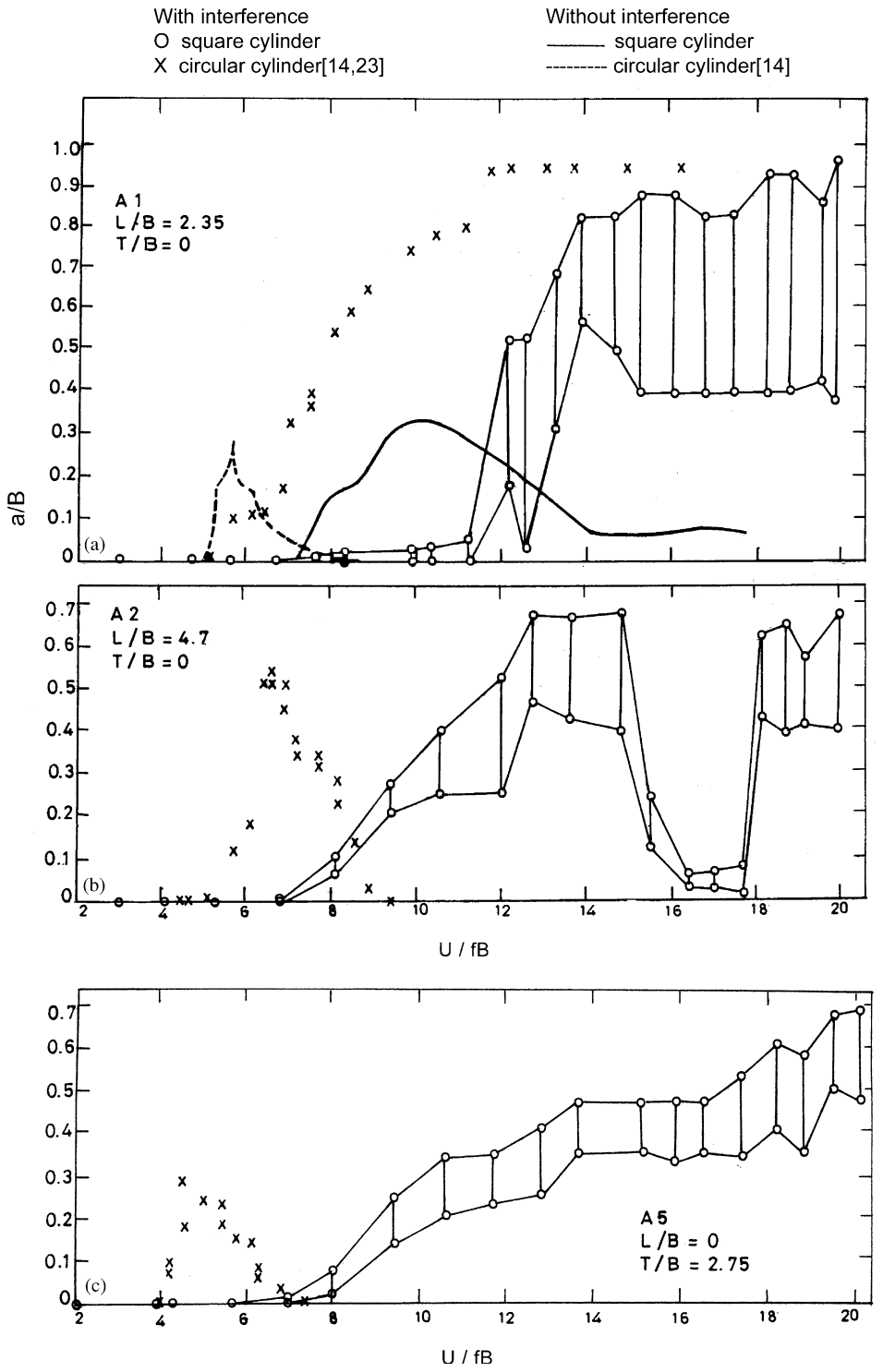

Fig. 7. Interference effects: $b/B = 2.0$. Reference position (see Fig. 1), L/B, T/B: (a) A1, 2.35, 0; (b) A2, 4.7, 0; (c) A5, 0, 2.75; (d) A6, 1.175, 2.05; (e) A7, 2.35, 1.30; (f) A9, 3.53, 0.65; (g) A14, 4.70, 2.75.

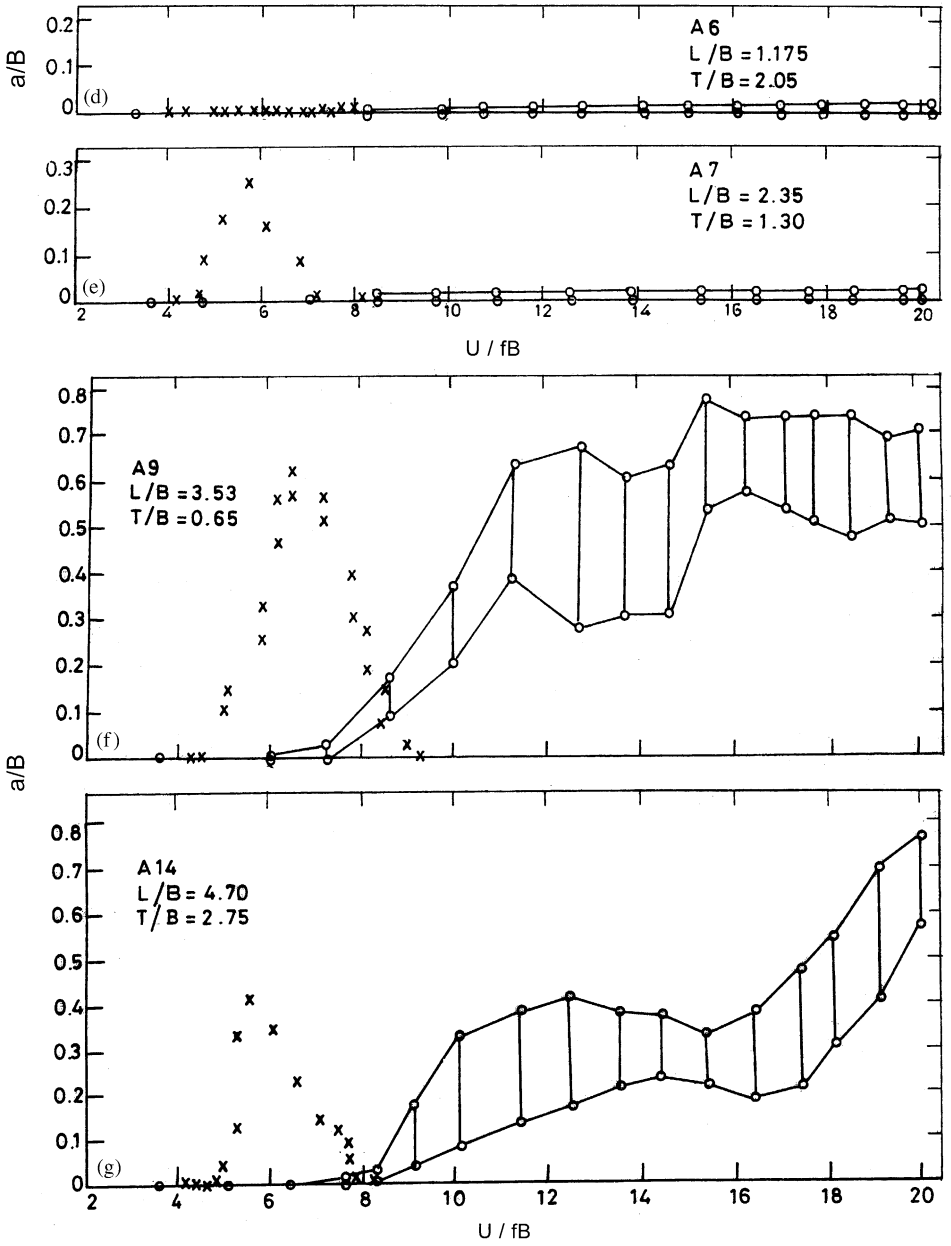

Fig. 7. (*Continued*)

levels persist. At position A7 (Fig. 5(d)), there is some increase in the peak amplitude value due to interference effects in the reduced velocity range $8.0 < U/fB < 14.0$, with a vibration suppression region in the reduced velocity range $14.0 \leqslant U/fB \leqslant 18.0$. For reduced velocities greater than 18.0, the amplitude of the test cylinder increases steeply to a large value and tends to remain so with further increase in reduced velocity. Circular cylinder exhibits in general, reduced amplitude levels compared to that of square cylinder at positions A6 and A7. The test cylinder response at positions A2, A3, A5, A9, A10, A11, A12, A13 and A14 are, in general, very similar to that of the single cylinder case with marginal differences in the amplitude level and hence the results for A12 (Fig. 5(e)) only are presented. However, the interference effects are seen to be marked in all these positions for the circular cylinder.

3.2.3. Results for $b/B = 1.5$

For $b/B = 1.5$, the interference effects are very severe at A1 (Fig. 6(a)). The maximum amplitude value is nearly two times that of the no-interference case (Fig. 6(a)). The oscillation of the test cylinder starts at a slightly higher value of reduced velocity (around $U/fB = 8.0$) compared to single cylinder case (Fig. 6(a)) and increases to a very high value ($(a/B)_{max} = 0.66$, reached at $U/fB = 13.0$). The amplitude remains same with further increase in the reduced velocity i.e., shows no tendency to return to lower amplitude levels. Beyond $U/fB = 14.0$, it was noticed that the difference between the maximum and minimum amplitude values (in the amplitude band) increases, as U/fB increases. The behaviour of the amplitudes returning to low values with increase in reduced velocity is typical of vortex-induced oscillations and the mechanism responsible for the response seen in Fig. 6(a) can be expected to be different. Further, it is interesting to observe that for the circular cylinder, for the case of $d/D = 1.5$, although the amplitude reached is quite high, there is a finite region of resonance which extends up to $U/fB = 12.0$. However, for square section cylinder, with the same relative size i.e., $b/B = 1.5$, there is no such finite region of resonance observed and the amplitudes continue to have large values with increasing reduced velocity. At position A2 (Fig. 6(b)), the test cylinder exhibits an increasing-decreasing trend of amplitude in the reduced velocity range $8.0 \leqslant U/fB \leqslant 20.0$, with a dip of amplitude at around $U/fB = 15.0$. The response of the test cylinder is considerably different even in the trend when compared to the no-interference case. Circular cylinder exhibits very high peak amplitude value at this position (almost equal to that of square cylinder), but the overall trend is much different compared to the square cylinder. At position A5 (Fig. 6(c)), the test cylinder amplitude exhibits an increasing-decreasing trend up to $U/fB = 12.0$ and thereafter a continuously increasing trend. Square cylinder vibrations far exceeds that of circular cylinder at this position. At position A6 (Fig. 6(d)), the test cylinder vibrations are completely suppressed over the entire range of reduced velocity tested, whereas, circular cylinder exhibits very small amplitude of vibration. At position A7 (Fig. 6(e)), it is observed that the vibrations are almost completely suppressed up to a reduced velocity of 14.0, beyond which the amplitudes are seen to increase sharply and continuously with U/fB. Even at a reduced velocity of 20.0, significantly high amplitudes persist ($(a/B)_{max} = 0.7$). At this position, vibrations are found to be less vigorous for the circular cylinder than those for the square cylinder. At position A11 (Fig. 6(f)) which falls in the wake-interference region, there is an initial range of U/fB where, the amplitude increases and reaches a peak value. With further increase in U/fB, the amplitude remains nearly the same. Circular cylinder exhibits considerably high vibrations at this position. Even in the no-interference region, at position A14, test cylinder exhibited vigorous vibrations as shown in Fig. 6(g). Once initiated, the amplitude shows an overall continuously increasing trend (Fig. 6(g)).

Response characteristics of the test cylinder at positions A3 is found to be nearly the same as that of the single cylinder case (Fig. 3). Test cylinder response at position A4 is almost the same as that at A6. Also, at positions A9, A10 and A12, the test cylinder exhibited similar responses as that at position A14. Hence, these are not shown here.

3.2.4. Results for $b/B = 2.0$

Among all the cases considered, the most severe effects are seen for the case of $b/B = 2.0$, particularly in the tandem position A1 (Fig. 7(a)). The features are similar to those observed for $b/B = 1.5$ at this position, but with considerably higher maximum amplitude value (nearly three times that of the no-interference case) and the onset of oscillations occurring at a higher U/fB value (at around $U/fB = 11.0$). For $U/fB > 14.0$, a substantial increase can be noticed in the difference between the maximum and minimum amplitude values (during multiple amplitudes of motion), when compared to the case of $b/B = 1.5$. At this interference location, circular cylinder also exhibits substantially high amplitudes with similar trend as that of square cylinder (the maximum amplitude values are almost equal for both the geometries). At other tandem location A2 (Fig. 7(b)), the amplitude follows an increasing-decreasing trend at first followed by a vibration suppression region (for the range of reduced velocity $16.0 \leqslant U/fB \leqslant 18.0$). Then there is a sudden rise in the amplitude value; the maximum amplitudes are considerably higher when compared to the single cylinder case. For position A2 (Fig. 7(b)), even at a reduced velocity of 20.0, very high amplitude levels persist. At this location, circular cylinder also exhibits considerable amplitudes but lesser than that of the square cylinder. At position A5 (Fig. 7(c)), once initiated, the amplitude continuously increases with U/fB. At positions A6 and A7 (Figs. 7(d)–(e)), the test cylinder vibrations are completely suppressed due to the presence of the interfering

cylinder. For circular cylinder, oscillations are completely suppressed at location A6 but notable vibrations occur at A7. At position A9 (Fig. 7(f)), the test cylinder exhibits an increasing trend of amplitude, reaches a maximum; thereafter, the amplitude remains unchanged. At positions A11 and A12, vibratory trend of the test cylinder is similar to that at position A9 (and hence not shown). At position A14 also (which is in the no-interference region), considerable interference effects exist as Fig. 7(g) shows (at position A13, the test cylinder response is quite similar to that at A14 and hence, not shown).

In Figs. 8(a)–(d) are shown the contours of the magnification factor, M which is defined as

$$M = \frac{(a/B)_{\max} \text{ with interference}}{(a/B)_{\max} \text{ for isolated cylinder}}.$$

These plots can be utilised to get a reasonable estimate of the response of the test cylinder, for any desired position of the interfering cylinder. The orthographic views shown in Fig. 9 give a visual picture of the relative magnitude of the amplitudes, location of the peak amplitudes and how they are distributed for the different b/B values. It can be seen clearly from these views that, the range of spacings over which the interference effects are felt and the maximum amplitude occurring in close tandem position increase with b/B ratio. Figs. 8 and 9 were obtained by using the results at the 14 positions shown in Fig. 1. The values at other positions were obtained by interpolation; and hence, the values obtained from these figures will be of limited use. However, they do give an idea of the possible response of the test cylinder at various arrangements.

4. Discussion

The response of the test cylinder presented in the set of Figs. 4–7 can, in general be attributed to the influence of the interfering cylinder on the vortex shedding process and on the flow field around the former coupled with the change in the configuration of the shear layers. In this section, a detailed discussion is provided both on single cylinder case and on cases with interference.

4.1. Single cylinder case

In Fig. 3, is shown the vibratory response characteristics of a spring-mounted square cylinder, exposed to a uniform flow (details have been already presented in the Section 3.1). In this case, the Scruton number (k_s) is 3.2 and damping ratio (β) is 0.0006. The characteristic of response (Fig. 3) seems to be typical of vortex-induced oscillation. Parkinson and Smith [24] have presented results for a square cylinder under galloping, for different ratios of damping (β). They have also indicated in their results, the position of vortex resonance for these various damping ratios (β) varying from 0.00107 to 0.0032 and also the reduced velocity at which the galloping starts. Based on these, the reduced velocity range for the lowest damping value $\beta = 0.00107$ over which vortex excitation can occur turns out to be from 7.0 to 15.0. This range agrees very satisfactorily with the range of vortex excitation observed in the present study. However, the value of Scruton number for $\beta = 0.00107$ in Parkinson and Smith's study works out to be 15.6, whereas in the present study, it is only 3.2. This could be the primary reason for Parkinson and Smith [24] not to have observed the vibratory response observed in the present study over the range of reduced velocity in the vortex excitation range.

For a square-section cantilever beam with a damping ratio of around 0.005, Olivari [6] has reported a vortex excitation range of $7.0 \leqslant U/fB \leqslant 13.0$, with it's overall response typical of resonance under vortex excitation. However, no multiple amplitudes have been reported unlike in the present study. But the amplitudes reported are rms. values indicating possible variation about a mean. Further, the cantilever condition seems to lead to higher magnitudes of vibration amplitude compared to the present study.

In the oscillatory response behaviour of an isolated square section cylinder reported by Takeuchi and Matsumoto [9] (referred to as T&M in the future) where the Scruton number is 2.4, the square cylinder is seen to exhibit a galloping type of response (a continuously increasing trend of amplitude followed by a constant amplitude trend). In the present study, relatively higher value of k_s (= 3.2) appears to be the reason for the amplitudes to reduce after reaching a peak value, the overall trend being that for vortex excitation.

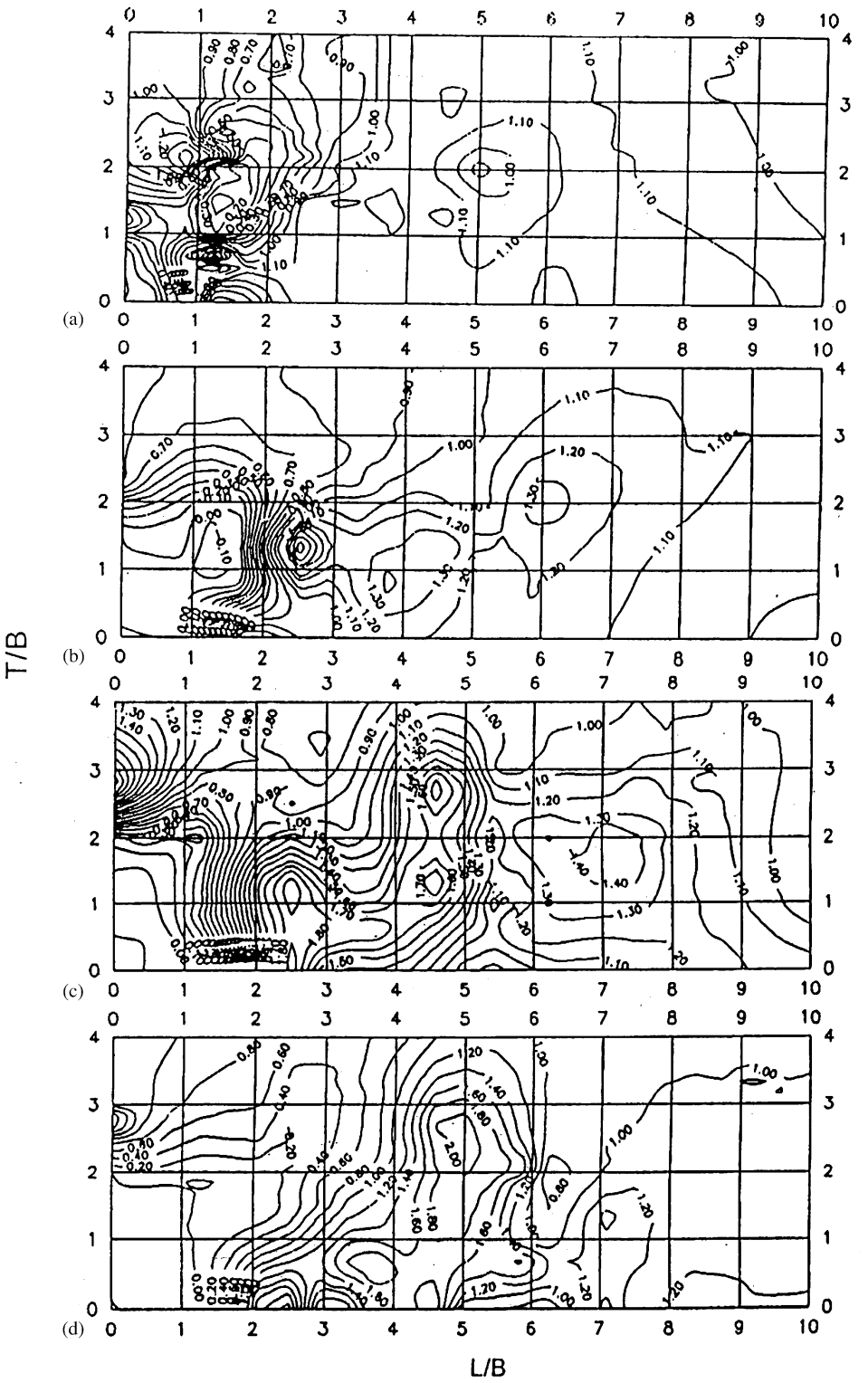

Fig. 8. The contours of the magnification factor M: (a) $b/B = 0.5$, (b) $b/B = 1.0$, (c) $b/B = 1.5$ and (d) $b/B = 2.0$.

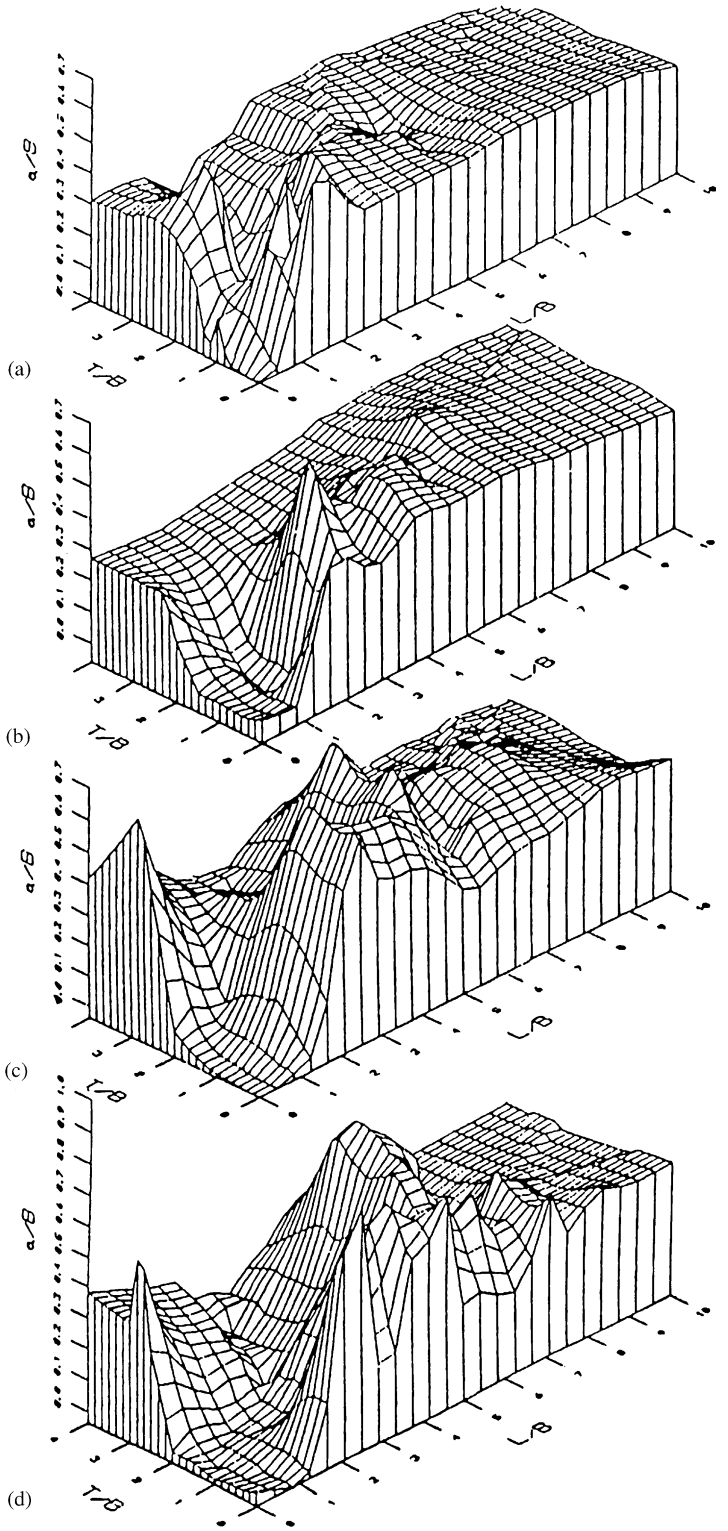

Fig. 9. An orthographic view of oscillatory response: (a) $b/B = 0.5$, (b) $b/B = 1.0$, (c) $b/B = 1.5$ and (d) $b/B = 2.0$.

4.2. Interference cases (vibratory response)

In Fig. 4(a), is shown the response of the test cylinder (with interference) for $b/B = 1.0$, at the tandem location with $L/B = 2.35$. The vibratory trend observed is an increasing-decreasing one, with $(a/B)_{max} = 0.45$, at around $U/fB = 12.0$. At nearly the same tandem location ($L/B = 2.75$), T&M have given the vibratory response of the upstream cylinder (shown in Fig. 3(a) in their paper). They have used two spring-mounted square cylinders in their interference experiments, the Scruton number for both the cylinders being 2.4. The non-dimensional maximum amplitude value (peak-to-peak) noticed in their case is only 0.16 (much less than the present case value of 0.45). Similar to the present study, they also have observed amplitude variation within a low and high peak. At $L/B = 3.0$, they have observed a substantial increase in the amplitude the trend remaining the same as at $L/B = 2.75$; the maximum non-dimensional amplitude value noticed is 0.52 (close to the present study). Amplitude bands are indicated at some values of U/fB.

As mentioned earlier, at position A1 ($L/B = 2.35$, $T/B = 0$) for $b/B = 1.5$ and 2.0 (Figs. 6(a) and 7(a)) and $U/fB > 14.0$, the test cylinder is observed to execute very vigorous oscillations. This occurs with a continuous increase of amplitude once the vibrations are triggered, followed by a nearly constant amplitude trend. Gowda and Sreedharan [14] have observed similar response for circular cylinder for the size ratio $d/D = 2.0$ where, the upstream cylinder is flexibly mounted (and rigid) and the interfering cylinder is rigid (and fixed) similar to the present study. They argued that this is due to proximity-induced galloping as observed by Bokain and Geoola [25]. Bokain and Geoola [25] have observed proximity-induced galloping for circular cylinders in close spacings characterised by an initial steep increase of amplitude followed by either a gradual increase of amplitude or a nearly constant amplitude trend. Hence, in the present case also (i.e., for square cylinder), it is logical to expect the behaviour of the test cylinder to be due to proximity-induced galloping.

Considering the various responses under the varying velocity case shown in Figs. 4–7, it can be observed that in many cases the response characteristics of the test cylinder show an initial increasing-decreasing trend (characteristic of vortex induced oscillations) followed by galloping type of excitation (such as at positions A6 and A7 for $b/B = 0.5$; at positions A2 and A3 for $b/B = 2.0$) where, the two kinds of oscillations are clearly separated. In other cases, the test cylinder has exhibited either vortex induced oscillations (such as in the case of $b/B = 0.5$, for positions A1, A2, A3 and A5) or proximity-induced galloping type of oscillations such as at position A7 for $b/B = 1.0$ and A1 for $b/B = 1.5$ and 2.0. As mentioned earlier, for square cylinder, multiple amplitudes are seen to occur in all the cases of interference as with single cylinder case.

4.3. Flow visualisation results

Flow visualisation experiments were carried out for the various arrangements by using two solid square cylinders to obtain some insight into the changes in the flow field that occur and their possible influence on the observed response of the test cylinder. The fluid used is water, and fine aluminium powder was used as tracer particles. Experiments were conducted at a Reynolds number of 5200 (with the test cylinder side dimension of 30 mm) which corresponds to the reduced velocity at the peak amplitude of the single cylinder (Fig. 3). Tests were conducted for different b/B ratios: i.e., 0.5, 1.0, 1.5 and 2.0. The results at only two positions are presented in Figs. 10–12. Flow visualisation experiments were carried out at different b/B ratios with the following conditions: (a) when both the cylinders are stationary and rigid, (b) when one of the cylinders is oscillated to simulate the vibratory condition. A video was also taken in the later case to capture the flow field at various instances in the vibratory path of the oscillated cylinder (but not presented here). All these studies have been carried out at a velocity which gives a reduced velocity of $U/fB = 10.0$. This could be considered as a limitation, as the vibratory response at positions A1 to A14 extend over a range of velocities. Inspite of this limitation, the results do give a better physical insight in to the features of the flow induced vibratory phenomenon. In what follows, these results are presented and discussed. To bring out interference effects more clearly, flow fields around a single square cylinder in stationary and vibrated conditions are also given (Figs. 10(a) and (b)). For the case with vibrated cylinder, to sense the direction of motion of the cylinder, an L.E.D encased in a rubber ball is made use of (can be seen placed just to the left hand side of the square cylinder in the photographic plates presented.). An electric circuitry has been made so that in one direction, the L.E.D will on 'on' and in the other direction, it will be 'off'.

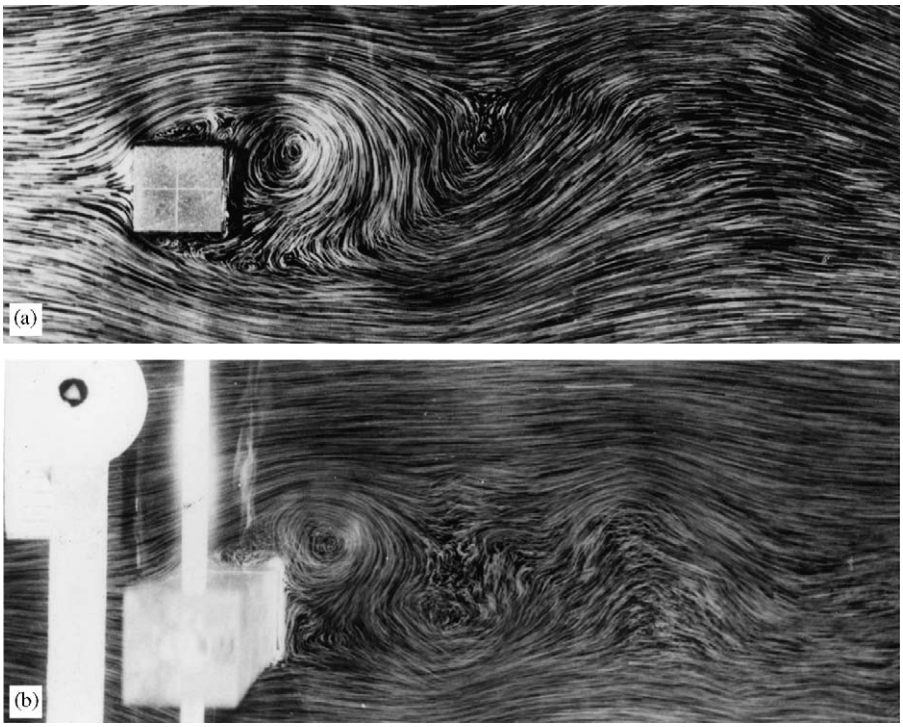

Fig. 10. Typical flow patterns around a square cylinder: (a) stationary cylinder and (b) oscillated cylinder.

The flow visualisation results are presented in the form of photographic plates for the cases with stationary and vibrated cylinder (where, instantaneous flow patterns around the cylinder can be observed at a particular vibratory position).

The results for arrangement A6, which is in the proximity-interference region, are shown in Figs. 11(a)–(d), with stationary front cylinder. It is observed that as the relative size of the cylinder (b/B) is increased from 0.5 to 2.0, the strength of the gap flow increases and its bias towards the upstream cylinder (which corresponds to the test cylinder in air experiments) also increases. This is particularly so for $b/B = 1.0$, 1.5 and 2.0. Under such a condition, the wake of the front cylinder is considerably narrowed down. It can be observed that in all these cases, the gap flow disrupts the vortex shedding process from the front cylinder (vortices are pushed away from the base region of the test cylinder by the gap flow). This situation leads to substantial reduction in the lift force on the front cylinder, which is well reflected in the oscillatory response of the test cylinder shown in Figs. 4(f), 5(c), 6(d) and 7(d) for different b/B ratios. It is seen that the response amplitude values for all the b/B ratios except for $b/B = 0.5$ are quite negligible (For $b/B = 0.5$ (Fig. 11(a)), it could be seen that, appreciable vortex shedding takes place from the upstream cylinder which is reflected in the amplitude of vibration of the test cylinder.).

In Fig. 12(a)–(c), are shown the flow patterns around the oscillated front cylinder for $b/B = 0.5$, 1.0 and 1.5 at position A7 ($L/B = 2.35$, $T/B = 1.3$) where, the test cylinder occupies the mean vibratory position. It is evident from the figure that, as the b/B ratio increases, the gap flow increases and becomes more biased towards the cylinder (upstream) reducing the wake width and disrupting the vortex shedding process. Hence, reduction of amplitude can be expected as b/B ratio increases. For $b/B = 0.5$, it can be observed (Fig. 12(a)) that significant vortex shedding takes place from the front cylinder with vortex size larger (implying larger quantum of circulation contained in it) than that of the oscillated single cylinder case (Fig. 10(b)). This extends a possibility of higher lift force generation and consequent higher amplitude of vibration. Correspondingly, $(a/B)_{\max} = 0.42$ (Fig. 5(d)). For $b/B = 1.0$, the wake width is narrower when compared to the case with $b/B = 0.5$. Also, the vortex size can be observed to be nearly identical to that of the oscillated single cylinder case (Fig. 10(b)). This indicates that considerable lift generation is possible leading to nearly equal amplitude

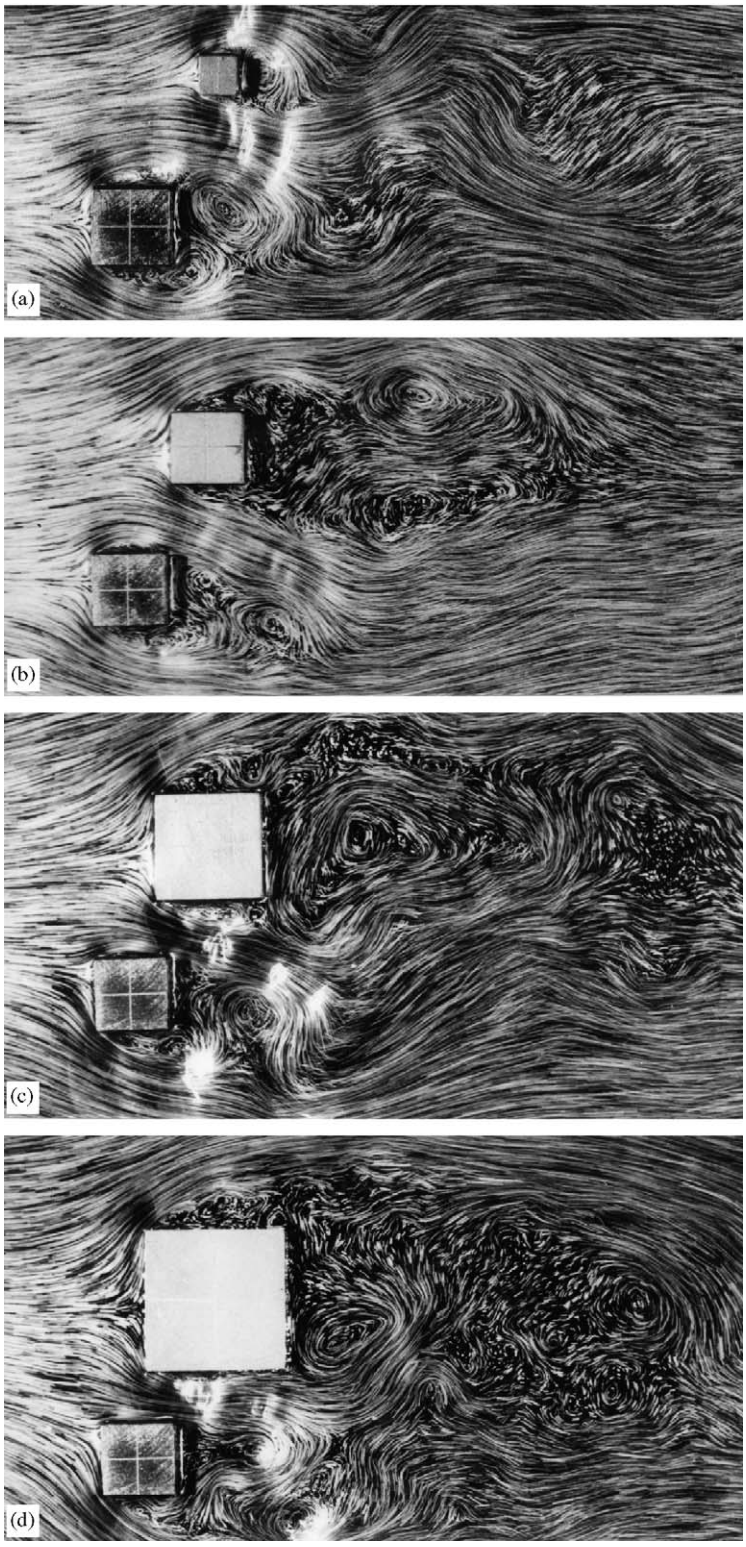

Fig. 11. Flow patterns for arrangement A6 ($L/B = 1.175$, $T/B = 2.05$) with stationary front cylinder: (a) $b/B = 0.5$, $(a/B)_{max} = 0.20$; (b) $b/B = 1.0$, $(a/B)_{max} = 0.01$; (c) $b/B = 1.5$, $(a/B)_{max} = 0.01$; (d) $b/B = 2.0$, $(a/B)_{max} = 0.01$.

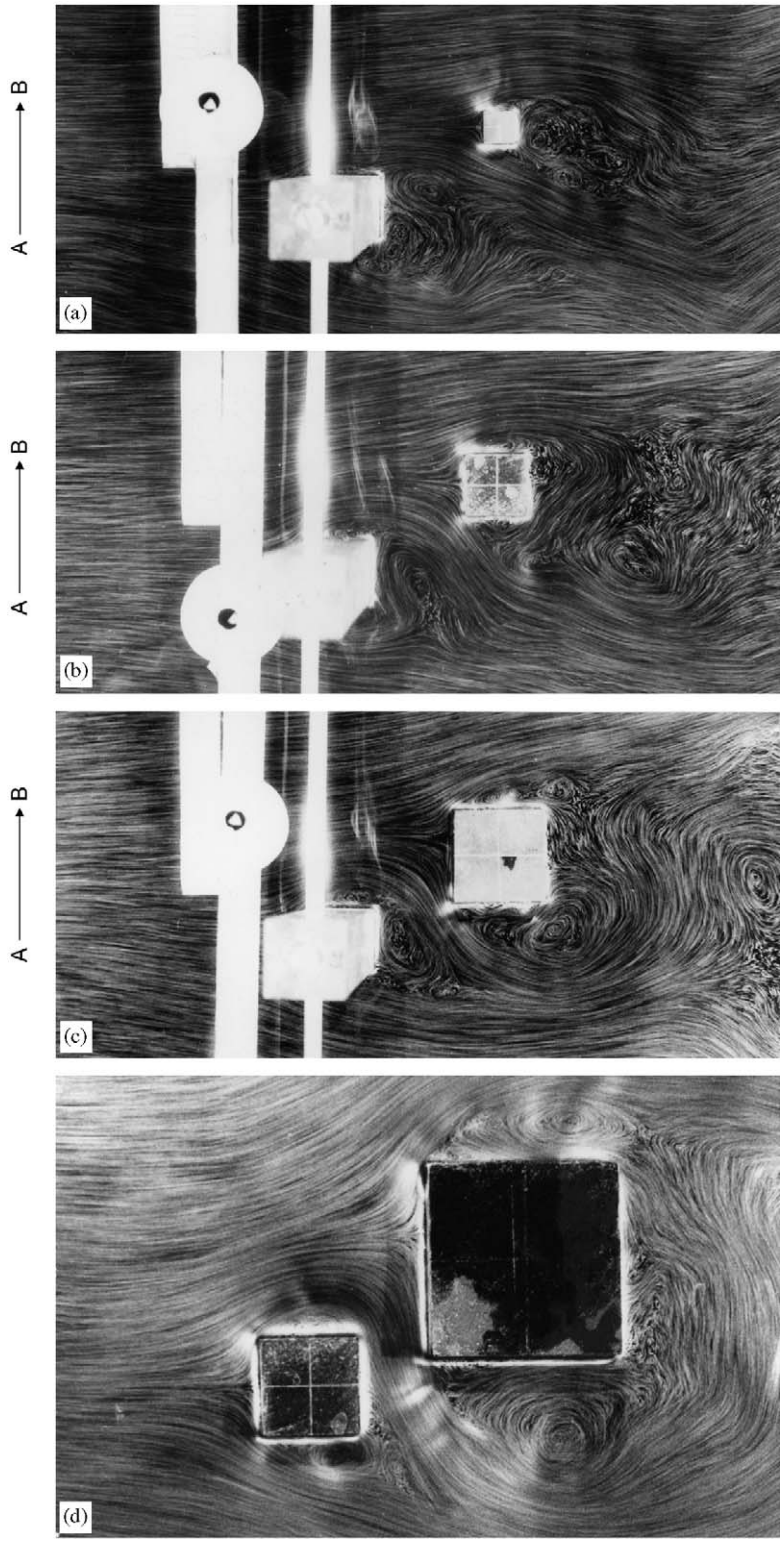

Fig. 12. Flow patterns for arrangement A7 ($L/B = 2.35$, $T/B = 1.30$) with oscillated front cylinder occupying the mean position (dir. AB): (a) $b/B = 0.5$, $(a/B)_{max} = 0.42$; (b) $b/B = 1.0$, $(a/B)_{max} = 0.31$; (c) $b/B = 1.5$, $(a/B)_{max} = 0.03$; (d) $b/B = 2.0$, $(a/B)_{max} = 0.02$.

of vibration in both cases. For $b/B = 1.0$, $(a/B)_{max}$ value is 0.31 (Fig. 4(g)) which is close to that for the single cylinder case (where, $(a/B)_{max} = 0.32$). Hence, it appears that the flow pattern around the oscillated front cylinder substantiates the vibratory response.

For $b/B = 1.5$, wake width has further narrowed together with reduction in the vortex size (Fig. 12(c)). It is seen that the rolling up process of shear layers is adversely affected by the presence of the interfering cylinder. Hence, only substantially reduced amplitudes can be expected to result. Correspondingly, in this case $(a/B)_{max} = 0.03$ (Fig. 6(e)).

For $b/B = 2.0$, since the maximum amplitude value is too low ($(a/B)_{max} = 0.02$), the flow visualisation experiment with oscillated cylinder was not performed. For this case, it could be observed that (Fig. 12(d), where, the front cylinder is stationary), the wake width of the front cylinder is markedly reduced due to the strong gap flow occurring between the cylinders, significantly disrupting the vortex shedding process reflecting the substantially low amplitude value noticed.

The flow visualisation results presented in this section do offer a physical explanation to the observed vibratory response at various positions. However, the major limitation is that the results presented are at $U/fB = 10.0$ whereas, the vibratory response is obtained over a range of reduced velocities (this has been already pointed out in the beginning of the section).

5. Concluding remarks

From the results presented and discussed, it can be inferred that, due to interference effects, in the tandem arrangement, peak oscillatory amplitudes can be nearly three times that for the isolated cylinder. The magnification of the oscillations is not in general that severe for the side-by-side arrangement. In the staggered arrangement, position A9 gives rise to vigorous vibrations of the test cylinder (for $b/B = 2.0$) and the vibrations are almost suppressed in arrangement A6 for all the b/B ratios, except for $b/B = 0.5$.

There is a possibility of proximity-induced galloping when the gap between the cylinders is sufficiently small, as indicated by the response in the case of A1 for $b/B = 1.5$ and 2.0. Among all the situations considered, the tandem position A1 with $b/B = 2.0$ is found to give rise to the most severe conditions. In general, it is found that the vibratory amplitudes under identical conditions are higher for square geometry than for the circular geometry.

A tentative explanation based on the flow visualisation results (using both the cylinders, stationary and also with one cylinder oscillated and the other cylinder, stationary) in different arrangements has been offered to explain the response of the test cylinder in various cases. However, a theoretical modelling of the vibratory response of the test cylinder with interference would further explain some of the very interesting features observed in the present investigation.

References

[1] B.J. Vickery, Fluctuating lift and drag on a long cylinder of square cross-section in a smooth and in a turbulent stream, *Journal of Fluid Mechanics* 25 (1966) 481–494.

[2] B.R. Bostok, W.A. Mair, Pressure distributions and forces on rectangular and D-shaped cylinders, *Aeronautical Quarterly* 23 (1972) 1–6.

[3] Y. Otsuki, K. Washizu, H. Tomizawa, A. Ohya, A note on the aeroelastic instability of a prismatic bar with square section, *Journal of Sound and Vibration* 34 (1974) 233–248.

[4] Y. Nakamura, T. Mizota, Unsteady lifts and wakes of oscillating rectangular prisms, *Journal of Engineering Mechanics Division, Proceedings of the ASCE* 101 (EM6) (1975) 855–871.

[5] G. Parkinson, Phenomena and modelling of flow-induced vibrations of bluff bodies, *Progress in Aerospace Science* 26 (1989) 169–224.

[6] D. Olivari, An investigation of vortex shedding and galloping induced oscillation on prismatic bodies, *Journal of Wind Engineering and Industrial Aerodynamics* 11 (1983) 307–319.

[7] J. Blessmann, J.D. Riera, Wind excitation of neighbouring tall buildings, *Journal of Wind Engineering and Industrial Aerodynamics* 18 (1985) 91–103.

[8] H. Sakamoto, H. Haniu, Y. Obata, Fluctuating forces acting on two square prisms in a tandem arrangement, *Journal of Wind Engineering and Industrial Aerodynamics* 26 (1987) 85–103.

[9] T. Takeuchi, M. Matsumoto, Aerodynamic response characteristics of rectangular cylinders in tandem arrangement, *Journal of Wind Engineering and Industrial Aerodynamics* 41–44 (1992) 565–575.

[10] P.A. Bailey, K.C.S. Kwok, Interference excitation of twin tall buildings, *Journal of Wind Engineering and Industrial Aerodynamics* 21 (1985) 323–338.
[11] M.M. Zdravkovich, Flow induced oscillations of two interfering circular cylinders, *Journal of Sound and Vibration* 101 (1985) 511–521.
[12] B.H.L. Gowda, D.R. Prabhu, Interference effects on the flow-induced vibrations of a circular cylinder, *Journal of Sound and Vibration* 112 (1987) 487–502.
[13] B.H.L. Gowda, K.P. Deshkulkarni, Interference effects on the flow-induced vibrations of a circular cylinder in side-by-side and staggered arrangement, *Journal of Sound and Vibration* 122 (1988) 465–478.
[14] B.H.L. Gowda, V. Sreedharan, Flow-induced oscillations of a circular cylinder due to interference effects, *Journal of Sound and Vibration* 176 (1994) 497–514.
[15] P.W. Bearman, D.M. Trueman, An investigation of the flow around rectangular cylinders, *Aeronautical Quarterly* 23 (1972) 229–237.
[17] A. Okajima, Strouhal numbers of rectangular cylinders, *Journal of Fluid Mechanics* 123 (1982) 379–398.
[18] P.W. Bearman, E.D. Obasaju, An experimental study of pressure fluctuations on fixed and oscillating square section cylinders, *Journal of Fluid Mechanics* 119 (1982) 297–321.
[19] E.D. Obasaju, An investigation of the effects of incidence on the flow around a square section cylinder, *Aeronautical Quarterly* 34 (1983) 243–259.
[20] A. Laneville, Lu Zhiyong, Mean flow patterns around two dimensional rectangular cylinders and their interpretation, *Journal of Wind Engineering and Industrial Aerodynamics* 14 (1983) 387–398.
[21] S.C. Luo, Md.G. Yazdani, Y.T. Chew, T.S. Lee, Effects of incidence and after body shape on flow past bluff cylinders, *Journal of Wind Engineering and Industrial Aerodynamics* 53 (1994) 375–399.
[22] G.V. Parkinson, Wind-induced instability of structures, *Philosophical Transactions of the Royal Societ of London, Series A* 269 (1971) 395–409.
[23] V. Sreedharan, Interference effects on the flow-induced oscillations of a circular cylinder, MS Thesis, Indian Institute of Technology Chennai, Madras, 1992.
[24] G.V. Parkinson, J.D. Smith, The square prism as an aeroelastic non-linear oscillator, *Quarterly Journal of Mechanics and Applied Mathematics* 17 (1964) 225–239.
[25] A. Bokaian, F. Geoola, Proximity-induced galloping of two interfering circular cylinders, *Journal of Fluid Mechanics* 146 (1984) 417–449.